

## **GesSo: A Steerable Soft-Bodied Robot Based on Real-Time Gesture Control**

### **Supplementary Materials**

**J. Lai, B. Lu, K. Huang, and H. K. Chu**

**The Hong Kong Polytechnic University, Hong Kong**

[jw.lai@connect.polyu.hk](mailto:jw.lai@connect.polyu.hk); [henry.chu@polyu.edu.hk](mailto:henry.chu@polyu.edu.hk)

#### **Links:**

- Demo video 1: <https://youtu.be/C1NUdoweUs>
- Demo video 2: <https://youtu.be/-SZDHfevCCg>
- Demo video 3: [https://youtu.be/9-W7Ji7w2\\_o](https://youtu.be/9-W7Ji7w2_o)
- Robot Simulator: <https://github.com/samlaipolyu/GesSo>

### A. Robot Description

The dimension and assembly are shown in the figure below, and the physical properties are shown in the table below (note:  $E$  - Young's Modulus;  $I$  - second moment of inertia;  $K_a$  - axial stiffness;  $K_T$  - bending stiffness). Each soft segment was actuated by 3 cables. The proximal segment had 6 cable-passages, in which 3 of them were for the distal segment. A main hollow passage was spared at the core. The cable coupling design benefits a compact and miniaturized manipulator structure but requires real-time actuation decoupling for the valid control.

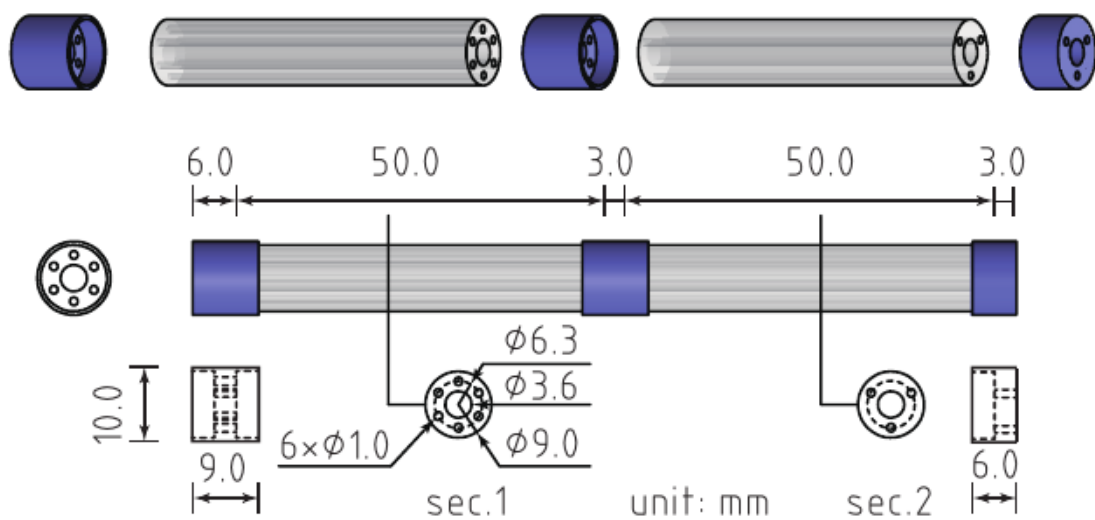


**Fig. S1:** Assembly of the 3-D printed cable-driven soft robot. The soft material (body parts) is Agilus30 PolyJet Photopolymer from Stratasys. The blue caps are made from PLA.

## PARAMETERS OF THE SOFT SEGMENT

$E$ [MPa]	$I$ [mm <sup>4</sup> ]	$K_a$ [Nmm <sup>-1</sup> ]	$K_T$ [Nmmrad <sup>-1</sup> ]	$L_k$ [mm]
0.8	313.8175	0.8550	5.0211–5.5790	50

**Table. T1:** Parameters of the soft segment

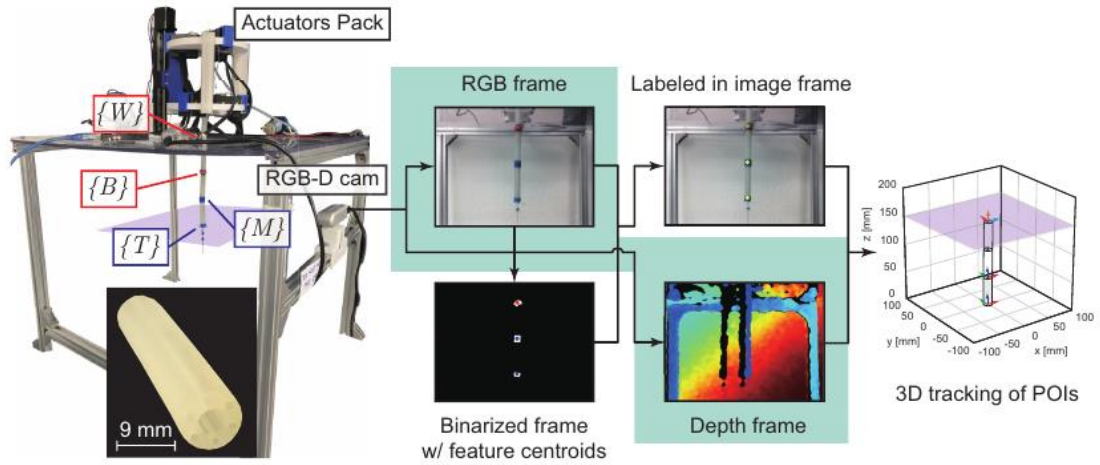


**Fig. S2:** Prototype setup and RGB-D processing for POIs tracking in 3-D.

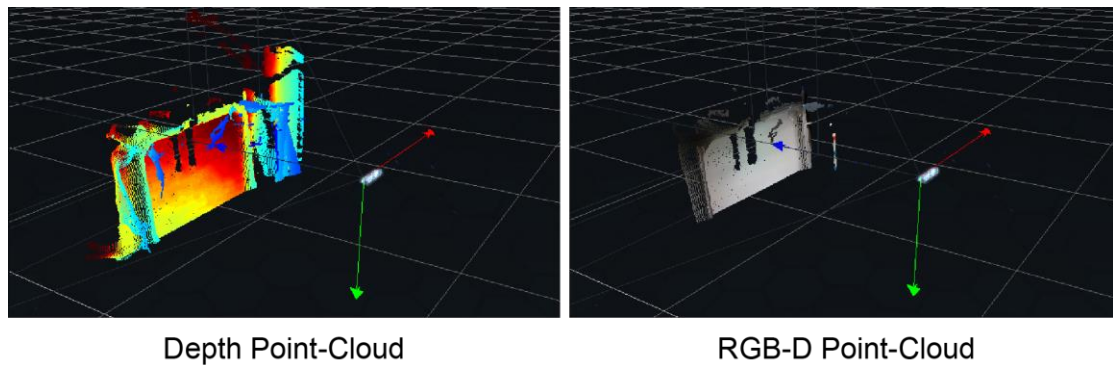


**Fig. S3:** Point-Cloud maps generated by the depth camera.

**B. Supplementary Content for Sec. V-B (Experiment for testing the Accuracy: Simulator v. Prototype)**

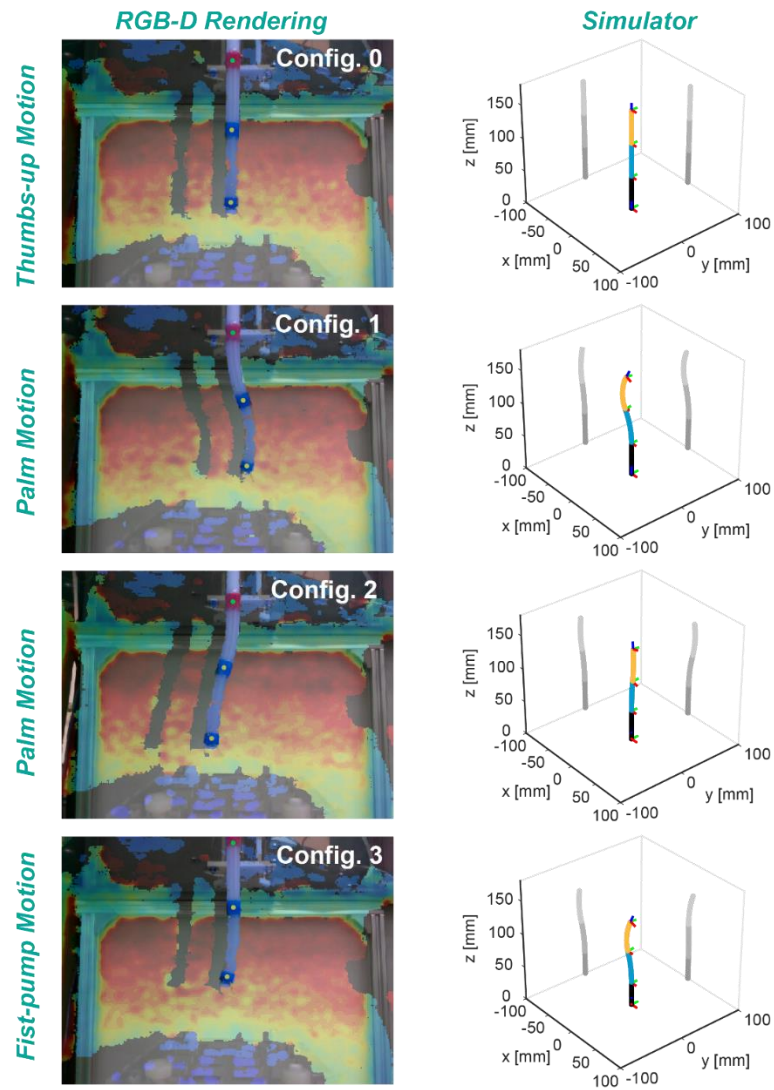


**Fig. S4:** (a-b) Different robot configurations (poses) for Table T1.

ERRORS BETWEEN SIMULATION AND EXPERIMENT OF THE POIs (UNIT: MM)

Position of POI w.r.t. $\{W\}$		$\{B\}$			$\{M\}$			$\{T\}$		
Axis <sup>†</sup>		X	Y	Z	X	Y	Z	X	Y	Z
Config. 0	sim.	0	0	50	0	0	100	0	0	150
	exp.	1.769	0	49.97	1.436	0	100.3	0.102	0	150.249
	err.	-1.769	0	0.03	-1.436	0	-0.3	-0.102	0	-0.249
Config. 1	sim.	0	0	48	-8.639	-3.296	97.56	7.475	-2.036	146.6
	exp.	1.674	0	46.38	-6.843	-5	97	7.401	-2	149.3
	err.	-1.674	0	1.62	-1.796	1.704	0.56	0.0740	-0.036	-2.7
Config. 2	sim.	0	0	44.36	6.467	-3.478	93.98	8.355	-4.397	143.9
	exp.	1.775	-1	44.19	6.042	-2	92.7	9.157	-5	143.5
	err.	-1.775	1	0.17	0.425	-1.478	1.28	-0.802	-0.603	0.4
Config. 3	sim.	0	0	40.19	-1.332	-4.908	90.2	6.280	-6.621	139.5
	exp.	1.697	-1	41.38	-2.127	-3	91.4	5.982	-6	139.4
	err.	-1.697	1	-1.19	0.795	-1.908	-1.2	0.298	-0.621	0.1

<sup>†</sup>The Y in exp. denotes the depth measurement from the RGB-D camera, with a resolution of 1 mm.

**Table T2: Errors between simulation and experiment of the POIs (unit: mm)**

We firstly examined the accuracy of tip positioning and the effectiveness of hand signal filtering by maneuvering the robot tip to (i) the desired spatial position for an 8-second stay, and (ii) the desired path as in the simulator. Hence, the error terms for evaluation could be defined as:

$$e_{\mathbf{x},exp} = \|\mathbf{x}_{T,sim}^W - \mathbf{x}_{T,mea}^W\|_2$$

$$e_{\Theta,exp} = \|\Theta_{T,sim}^W - \Theta_{T,mea}^W\|$$

The experiment results of (i) and (ii) are shown in Fig. S4(a-b) and (c-d), respectively. The results indicate that the real-time pose of the robot tip being visually measured could satisfactorily align with the prediction from the simulator. Therefore, the robot tip can be well-maneuvered as desired. In the steady-state, the norm positioning errors can be within 4 mm, and the pointing direction error within 5 degrees.

We have also evaluated the accuracy of the predicted manipulator's motion in free space. In order to do that, we measured the positional errors between the simulation and experiments of the POIs, namely,  $\{B\}$ ,  $\{M\}$ , and  $\{T\}$  with the concerning results shown in Table S1. Based on the specific gestures, different static configurations were posed as shown in Fig. S5. The results show that the deviations are within 3 mm on each axis. The errors may be caused by various factors, including gesture sensing (master side), prototype installation (follower side), and 3D measurement (evaluation side). Still, it can be concluded that our prototype robot could accurately reproduce the predicted motion from the simulator.

With that being said, a master-follower system does not necessarily be as highly accurate as the simulator, because the user could have the adjustment of gesture *in situ* based on subjective perception. Whenever the soft robot has interaction with the environment, without stiffness compensation, there is a high chance that the robot shall passively comply with the surroundings. Therefore, the robot maneuverability in task-space manipulation shall be examined.

### C. Supplementary Content for Sec. V-C (Experiment for testing the Maneuverability)

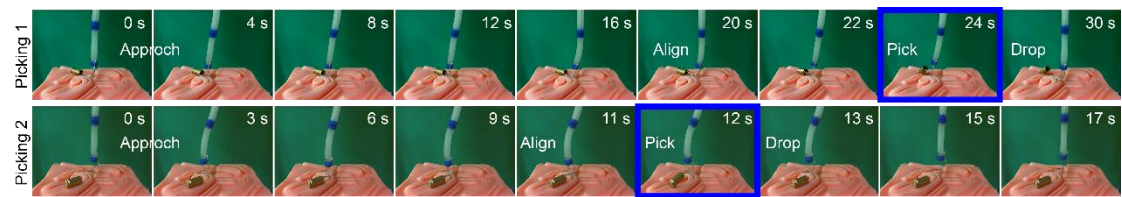


**Fig. S5:** Real-time master-follower manipulation: picking up a 9-mm bullet case in different locations on an uneven and sticky tissue phantom. (Images were captured from the supplementary video).

Since our robot was built for R-MIS, we have further conducted a series of laboratory trials to mimic the use of a soft robot in the MIS manipulation scenario. As shown in Fig. S6, a mental hook was attached to the robot tip, which was then used to pick up a small object on the uneven and sticky tissue phantom. The picking process involved (i) the approaching of tip to the object, (ii) the alignment of the hook and the bullet chamber, (iii) the action that lifts the bullet which was stuck on the phantom surface, and (iv) dropping. It shows that the examiner (a novice that has been trained for about 5 minutes) can successfully finish the picking tasks.

#### D. Hand Speed and Hardware Speed

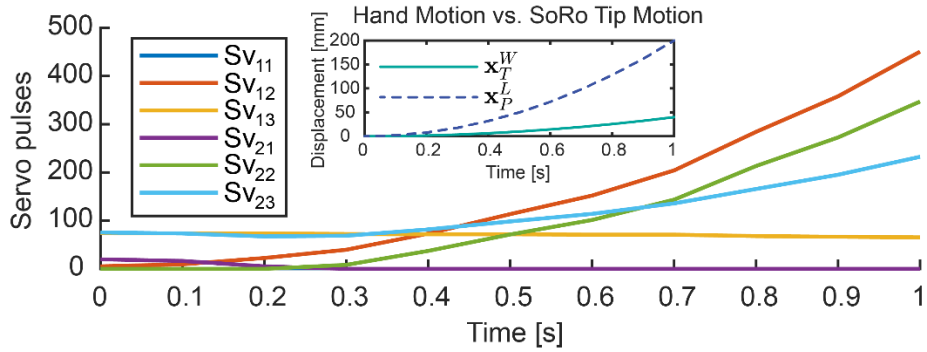


**Fig. S6:** The required servo pulses for cable actuation in a 1-second hand accelerated motion at  $400 \text{ mm/s}^2$ . No reduction gears were installed between the servos and cables.

We have analyzed the servo responses to the hand speed. It has been tested that, in general, the maximum speed our hand can reach in a limited space would be no more than  $400 \text{ mm/s}^2$ . As shown in Fig. S7, if a hand moves linearly from  $[0 \ 0 \ 120]$  mm to  $[40 \ 0 \ 120]$  mm with the palm orientation being  $[-0.9656 \ -0.1430 \ -0.2167]$  rad in an acceleration of  $400 \text{ mm/s}^2$  for 1 second, based on the computed IK, the maximum required servo pulse would be 450 pulses out of a 4096 pulses/rev. The maximum speed for a Dynamixel XM430-W350 servo is 3140 pulse/s at 12.0 V (<https://emanual.robotis.com/docs/en/dxl/x/xm430-w350/>), which is much greater than 450 pulse/s. A similar result can be attained for the slide motion (z-axis). It implies that - using the proposed steering method - the robot tip motion can be essentially synchronized to the hand motion at various speeds with the appropriate hardware selection.

## AUTHORS' BIO



**Jiewen Lai (S'20)** received the B.Eng. degree in metallurgical engineering from Wuhan University of Science and Technology, Wuhan, China, in 2016, and the M.Sc. degree in mechanical and automation engineering from The Chinese University of Hong Kong (CUHK), Hong Kong, in 2017. He is currently working toward the Ph.D. degree in mechanical engineering with The Hong Kong Polytechnic University, Hong Kong.

He was a recipient of the Best Paper Finalist Award of the 2019 IEEE International Conference on Robotics and Biomimetics. His research interests include soft/continuum robots, surgical robots, and robot intelligence.



**Bo Lu** received the B.Eng. degree in ship and offshore engineering from Dalian University of Technology, Dalian, China, in 2013, and the M.S. and Ph.D. degrees in mechanical engineering from The Hong Kong Polytechnic University, Hong Kong, in 2015 and 2019, respectively.

He is currently a Post-Doctoral Research Fellow with the T Stone Robotics Institute, The Chinese University of Hong Kong (CUHK) since 2019. He will be joining the School of Mechanical and Electrical Engineering, Soochow University, Suzhou, China, as an Associate Professor, in late 2021. His current research interests include medical robotics, computer vision, and surgical automation technique.



**Kaicheng Huang (S'20)** received the B.Eng. degree in automation from Shenzhen University, Shenzhen, China, in 2014, and the M.Sc. degree in mechanical and automation engineering from The Chinese University of Hong Kong (CUHK), Hong Kong, in 2015. He obtained his Ph.D. degree from the Department of Mechanical Engineering, The Hong Kong Polytechnic University, Hong Kong, in 2020.



He was a Post-Doctoral Fellow with the University of Hong Kong (HKU) from 2020 to 2021. He is currently a Post-Doctoral Fellow with Southern University of Technology (SUSTech), Shenzhen, China. His research interests include automated cell patterning, robotic control, and machine learning.



**Henry K. Chu (M'12)** received the B.S. degree in mechanical engineering from the University of Waterloo, Waterloo, ON, Canada, in 2005, and the M.ASc. and Ph.D. degrees from the University of Toronto, Toronto, ON, Canada, both in mechanical and industrial engineering, in 2007 and 2011, respectively.

He was the recipient of the top-ranked Canada Graduate Scholarship (CGS) (2009-2011) and the pre-approved candidate of the Industrial R\&D Fellowships (IRDF) program (2012) from the Natural Sciences and Engineering Research Council of Canada (NSERC). He was a Post-Doctoral Fellow with the University of Toronto and the City University of Hong Kong. He is currently an Assistant Professor with The Hong Kong Polytechnic University, Hong Kong. His research interests include robotic manipulation, vision-based control and automation, micro-system design, and tissue engineering.

**---END OF THIS DOCUMENT---**